Molecular Therapy
Nucleic Acids
Original Article

Generation of Genetically Stable Human Direct-Conversion-Derived Neural Stem Cells Using Quantity Control of Proto-oncogene Expression

Kwon Daekee,[1] Han Mi-Jung,[1] Ji Minjun,[1] Ahn Hee-Jin,[1] Seo Kwang-Won,[1] and Kang Kyung-Sun[1,2]

[1]Stem Cells and Regenerative Bioengineering Institute in Kangstem Biotech, Biomedical Science Building, #81 Seoul National University, Seoul 08826, South Korea; [2]Adult Stem Cell Research Center, College of Veterinary Medicine, Seoul National University, Seoul 08826, South Korea

As the human lifespan has increased due to developments in medical technology, the number of patients with neurological diseases has rapidly increased. Therefore, studies on effective treatments for neurological diseases are becoming increasingly important. To perform these studies, it is essential to obtain a large number of patient-derived neural cells. The purpose of the present study was to establish a technology that allows the high-efficiency generation of genetically stable, direct-conversion-derived neural stem cells (dcNSCs) through the expression of a new combination of reprogramming factors, including a proto-oncogene. Specifically, human *c-MYC* proto-oncogene and the human *SOX2* gene were overexpressed in a precisely controlled manner in various human somatic cells. As a result, the direct conversion into multipotent dcNSCs occurred only when the cells were treated with an MOI of 1 of *hc-MYC* proto-oncogene and *hSOX2* retrovirus. When MOIs of 5 or 10 were utilized, distinct results were obtained. In addition, the pluripotency was bypassed during this process. Notably, as the MOI used to treat the cells increased, expression of the *p53* tumor suppressor gene, which is typically a reprogramming hurdle, increased proportionately. Interestingly, *p53* was genetically stable in dcNSCs generated through direct conversion into a low p53 expression state. In the present study, generation of genetically stable dcNSCs using direct conversion was optimized by precisely controlling the overexpression of a proto-oncogene. This method could be utilized in future studies, such as *in vitro* drug screening using generated dcNSCs. In addition, this method could be effectively utilized in studies on direct conversion into other types of target cells.

INTRODUCTION

The human lifespan has increased globally with development in medical technology. As a result, the number of patients with neurological diseases has also rapidly increased.[1] Because neurological disease can lower a patient's quality of life significantly, research on effective medicines and therapies to treat and cure neurological diseases has become increasingly important. Notably, due to the differences in genetic background, specific drugs may react differently in individuals.[2] Therefore, it may be useful to perform *in vitro* drug screening using patient-specific neural cells to develop drugs that are optimal for that patient.[3] In summary, in order to study therapeutic agents and treatments for neurological diseases for a specific patient effectively, it is necessary to obtain a sufficient number of neural cells from that patient.

However, obtaining a sufficient number of neural cells from patients is challenging; therefore, a cellular reprogramming technique must be used. Cellular reprogramming technology is largely divided into somatic cell nuclear transfer (SCNT), induced pluripotent stem cell (iPSC) technology, and direct conversion.[4] The major disadvantage of SCNT is that it requires human oocytes, which can cause ethical issues. In contrast, iPSC technology introduces a transcription factor into somatic cells and induces cellular reprogramming through a pluripotent state. Notably, teratoma may form when transplanting iPSCs *in vivo*. The most recently developed of the three technologies, direct conversion is a means of introducing transcription factors into somatic cells that are suitable target cells.[5,6] This technique is a valuable alternative to SCNT and iPSC technology, because it does not require the use of eggs or require cells to go through a pluripotent state.

Human *c-MYC* (*hc-MYC*) proto-oncogene is an important transcription factor used in iPSC technology.[7–10] However, successful generation of direct conversion-derived neural stem cells (dcNSCs) through direct conversion has not been reported using the *hc-MYC* proto-oncogene in conjunction with *hSOX2* (MS).[11–13] Therefore, the objective of this study was to establish a method to generate genetically stable dcNSCs effectively, using direct conversion by precisely controlling the level of *hc-MYC* proto-oncogene expressed in somatic cells.

RESULTS

Optimization of Human Dermal Fibroblast-dcNSC Production Conditions by Controlling the Overexpression of a Proto-oncogene

To overexpress the proto-oncogene *hc-MYC* and general neural inducing transcription factor *hSOX2* in somatic cells, the pMXs

Received 28 February 2018; accepted 13 December 2018;
https://doi.org/10.1016/j.omtn.2018.12.009.

Correspondence: Kyung-Sun Kang, Adult Stem Cell Research Center, College of Veterinary Medicine, Seoul National University, Seoul 08826, South Korea.
E-mail: kangpub@snu.ac.kr

retroviral vector was used (Figure 1A). A retrovirus was produced from 293FT cells and concentrated from viral supernatants collected 72 h post-transfection. Concentrated retroviruses were titrated by serial dilution before use in a direct conversion experiment (Figures 1B–1D). When human dermal fibroblasts (hDFs) were infected with the retrovirus at MOIs of 1, 5, and 10, there were significantly more cells following infection with an MOI of 1 compared to those following infection with an MOI of 5 or 10 ($p < 0.01$) at 2 days post-infection (Figure 2A). In addition, direct conversion into a dcNSC-like morphology was observed only when an MOI of 1 was used and not an MOI of 5 or higher (Figure 2B). The hDF-dcNSCs produced by treating with a retrovirus MOI of 1 could be cultured both attached and in suspension (Figure 1E). The hDF-dcNSCs maintained dcNSC-specific morphology and proliferated following freezing and thawing as well (Figure 1F). Comparison and analysis of direct conversion efficiency based on expression of NSC marker CD133 found differences of 0.2%–0.5% in each hDF batch (Figure 1G).[14–16] As the MOI of retrovirus used to infect the hDFs increased, the transcript and protein expression level of *p53*, a major reprogramming hurdle, increased proportionally and significantly ($p < 0.01$ and < 0.05, respectively) (Figures 2C and 2D). In addition, it showed the pattern that, as MOI increased, the expression of an apoptosis marker (*BAX*) increased and the expression of a NSC marker (*PAX6*) decreased ($p < 0.01$ and < 0.05, respectively) (Figures 2E and 2F). The hDF-dcNSCs had significantly lower transcript expression level of *OCT-4*, a typical marker of pluripotency, than iPSC ($p < 0.01$) (Figure S1A). No significant change was observed when MS was introduced into hDF, and the expression level of pluripotency related gene was checked by time course (Figure S1B). In addition, if *hOCT-4* and *hKLF4* included in the iPSC technology of *hOCT-4*, *hSOX2*, *hc-MYC*, and *hKLF4* (OSMK) were excluded, alkaline phosphatase (AP)-positive colonies did not form, even if the transgenic cells were incubated in iPSC reprogramming-favorable conditions (Figure S1C). Fingerprinting revealed that hDFs were the parental origin of the hDF-dcNSCs (Figure 4A). Based on the transcript and the protein levels, these hDF-dcNSCs expressed endogeneous NSC-specific markers SOX2, NESTIN, and PAX6 (Figures 4B and 4C). These cells had a doubling time of approximately 21.3 h, were self-renewing, and were multipotent, as they could spontaneously differentiate into neurons and glia (astrocyte and oligodendrocyte) (Figures 4D, S2A, and S2B).

Generation of dcNSCs from Various Somatic Cells

In the present study, the universality of direct conversion conditions was evaluated using different somatic cell types, including patient-derived somatic cells (Figure 3). Human umbilical cord blood-derived mesenchymal stem cells (hUCB-MSCs) were used, which expressed the typical MSC marker patterns of HLA-ABC$^+$, HLA-DR$^-$, CD34$^-$, CD45$^-$, CD73$^+$, and CD105$^+$ (Figure 3A). When cells were treated with MS, with an MOI of 1, and direct conversion was induced, an attached dcNSC-specific colony morphology was observed (Figure 3B). The hUCB-MSCs underwent direct conversion at an efficiency of approximately 1.0%–2.4% (Figure 3C). The hUCB-MSC-dcNSCs expressed SOX2, NESTIN, and PAX6 and differentiated into a neuron-like morphology (Figures 4B, 4C, and S2B). Human Niemann-Pick Type C disease-derived dermal fibroblasts (hNPCDFs) have a point mutation in the NPC1 gene that results in the substitution of an isoleucine of the NPC1 protein, with a threonine (Figure 3D). The hNPCDFs were converted into a dcNSC-specific morphology by direct conversion at an efficiency of approximately 1.3% (Figures 3E and 3F). The hNPCDF-dcNSCs expressed NESTIN and PAX6, but not the fibroblast markers COL1A2 and S100A4 (Figures 4B and 4C). In addition, these cells could differentiate into neurons and glia (Figures 4D and S2B).

Genetic Stability of dcNSCs

The hDF-dcNSCs were considered genetically stable on a macroscopic level, based on their normal karyotype (46, XX) (Figure 5A). In order to test for *p53* mutations, which should be avoided as an important safeguard against the cancerization of cells, the *p53* locus was amplified using hDF and hDF-dcNSC cDNA (Figure 5B). Sequencing of the resulting PCR product revealed no mutations in all six *p53* gene mutation hotspots (Figure 5C). Ten TA-cloned PCR products were individually sequenced to exclude the possibility of a mutation in *p53* in very few cells, and no mutations were found (Figure 5D).

DISCUSSION

In this study, MS was successfully utilized to generate dcNSCs using direct conversion technology. Specifically, precise control of retroviral MOI allowed direct conversion to occur effectively, where an MOI of 1 was optimal. Effective direct conversion at an MOI of 1 occurred as a result of overcoming the p53 reprogramming hurdle, and pluripotency appears to have been bypassed during conversion. This protocol is also applicable to adult stem cells and patient-derived cells, and the final product—i.e., dcNSCs—is genetically stable.

In cellular reprogramming studies using iPSC technology, the *hc-MYC* proto-oncogene has been successfully utilized.[7–10] The *MYC* proto-oncogene plays a role in increasing self-renewality of neural progenitors through Miz-1-mediated signaling transduction.[17] However, numerous direct conversion studies have failed to generate dcNSCs using the *hc-MYC* proto-oncogene.[11–13] In most studies, direct conversion was possible up to the induced neuron stage but failed at the dcNSC stage. However, this study successfully performed direct conversion of human somatic cells into dcNSCs using MS (Figure 1E). This direct conversion protocol can be used on not only hDFs but also hUCB-MSCs and hNPCDFs (Figure 3). Interestingly, direct conversion of somatic cells into dcNSCs occurred only when MS was delivered at a specific MOI (Figure 2B). In addition, it was confirmed by fingerprinting experiment that dcNSCs were derived by introducing the MS of a specific MOI into parental somatic cells, which means that there was no contamination of other cells during direct conversion process (Figure 4A).

The results of this study show that direct conversion of somatic cells into dcNSCs occurs when MS is delivered at an MOI of 1 but not an MOI of 5 or 10 (Figure 2B). This suggests a link with p53 expression, a

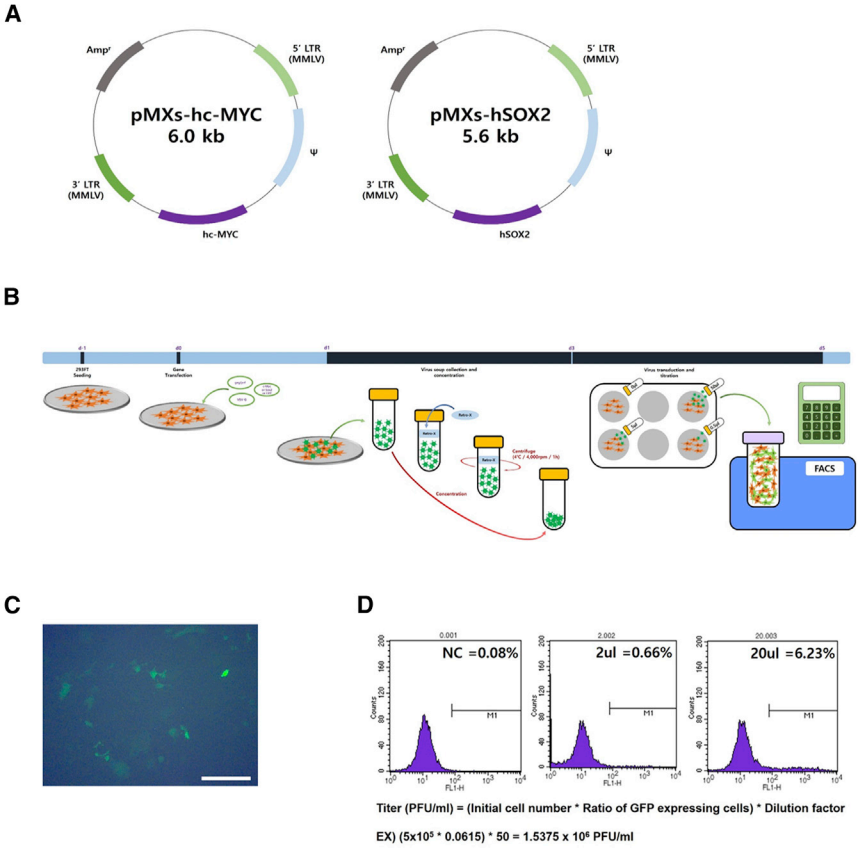

Figure 1. Direct Conversion of hDFs into dcNSCs through Novel Combination of the Transcription Factors *hc-MYC* and *hSOX2*

(A) Map of *hc-MYC* proto-oncogene and *hSOX2* retroviral vector used in human dcNSC generation through direct conversion. (B) Schematic representation of retrovirus production and titration. (C) GFP expression in 293FT cells 2 days post-transfection, with reporter GFP retroviral vector. (D) Retrovirus titration calculation using serial dilution method. (E) Formation of dcNSC-like colonies and neurospheres following the transduction of a combination of *hc-MYC* and *hSOX2* at an MOI of 1. (F) Morphology of hDF-dcNSCs after thawing. (G) Direct conversion efficiency of 3 hDF lines. Scale bars, 200 μm.

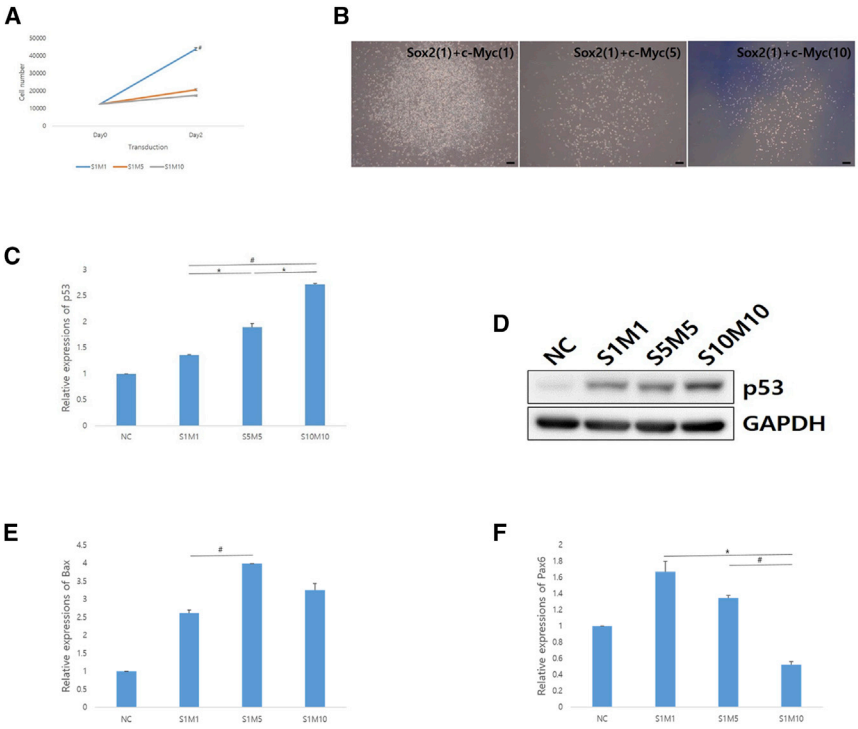

Figure 2. Optimization of Conditions for Direct Conversion of hDFs into dcNSCs through MOI-Mediated Control of *hc-MYC* and *hSOX2*

(A) Difference in cellular proliferation following the transduction of a combination of *hc-MYC* proto-oncogene and *hSOX2* into hDFs with MOIs of 1, 5, and 10. (B) Difference in hDF cell shape during early stage of direct conversion according to MOI. (C and D) Differences in *p53* transcript (C) and protein (D) expression levels during early direct conversion following treatment with different MOIs. (E) Difference in expression level of apoptosis marker according to MOI (10th day of transduction). (F) Difference in expression level of NSC marker according to MOI (10th day of transduction). *$p < 0.05$; #$p < 0.01$. Scale bars, 200 μm.

major reprogramming hurdle, which increases when the foreign gene is introduced into the cells at a high MOI (Figures 2C and 2D). The increase in *p53* gene expression proportionally with MOI is due to a homeostasis-maintenance mechanism that maintains genomic integrity in the cells.[18,19] Therefore, precise control of an MOI of 1 is considered critical for a high-efficiency direct conversion. However, in the previous studies of direct conversion from somatic cells into dcNSCs, there are many cases of no information about virus titration or cell-treated MOI. This may hinder the reproducibility of the experiments; therefore, titration must be performed after virus production to ensure that the correct amount of virus is introduced into somatic cells (Figures 1A–1D). In this study, direct conversion into dcNSCs was observed only at a relatively low MOI of 1 and not at MOIs of 5–20 that are generally used in cellular reprogramming using iPSC technology.[20,21] This phenomenon arises probably due to the exposure of the cells to NSC-specific complete serum-free defined conditions, immediately after virus transduction, and the cells might react very sensitively to MOI. Further research is required to identify a serum alternative, such as serum replacement, to make the experiment less sensitive to MOI.

It seems that pluripotency is bypassed during direct conversion into dcNSCs. In the dcNSCs that were generated in this study, *OCT4* transcript levels were similar to those in NSCs differentiated from ESCs and significantly lower than those in undifferentiated iPSCs (Figure S1A). During the reprogramming process, the pluripotency-related transcript (*OCT4* and *REX1*) did not increase significantly (Figure S1B). In addition, when only two factors of OSMK were excluded, no AP-positive colonies were obtained by iPSC reprogramming (Figure S1C). In other studies, it was reported that iPSC reprogramming occurs even if one or more OSMK factors are omitted, although the efficiency is very low.[22,23] The difference in the results obtained in this study are likely due to the low initial number of cells (1.25×10^4 cells) used, compared to the other group, which used 4- to 8-fold more cells ($5–10 \times 10^4$). In summary, the direct conversion conditions used in the present study are clearly unfavorable for entering a pluripotent state. Only two reprogramming factors (MS) were used in this study, compared to four (OSMK), and the MOI of 1 was much lower than an MOI of 5–20, which is generally used in iPSC reprogramming. In addition, complete serum-free defined medium and feeder-free conditions were used. Based on the results of this study and additional considerations, it is reasonable to assume that the cells bypassed the pluripotent state and phenotypically converted directly into dcNSCs, which were the target cell type.

There have been many reports on iPSC technology and direct conversion, suggesting that a decrease in the expression levels of *p53* tumor suppressor gene during reprogramming can lead to an increase in the reprogramming efficiency.[24–26] However, to our knowledge, no study has been conducted to test the genetic stability of *p53* at the DNA level in reprogrammed cells generated by controlling p53 level. This study experimentally demonstrates how relatively low p53 expression levels induced by treatment with a low MOI of MS affects *p53* gene expression in reprogrammed cells. As a result, the *p53* tumor suppressor gene in dcNSCs generated by precisely controlling MS MOI maintained stability at the DNA level (Figures 5C and 5D).[27–29] This study revealed MOI-mediated control of reprogramming factors as a new method of safely lowering p53 levels during reprogramming.

In conclusion, genetically stable dcNSCs were generated at a high efficiency using direct conversion by precisely controlling

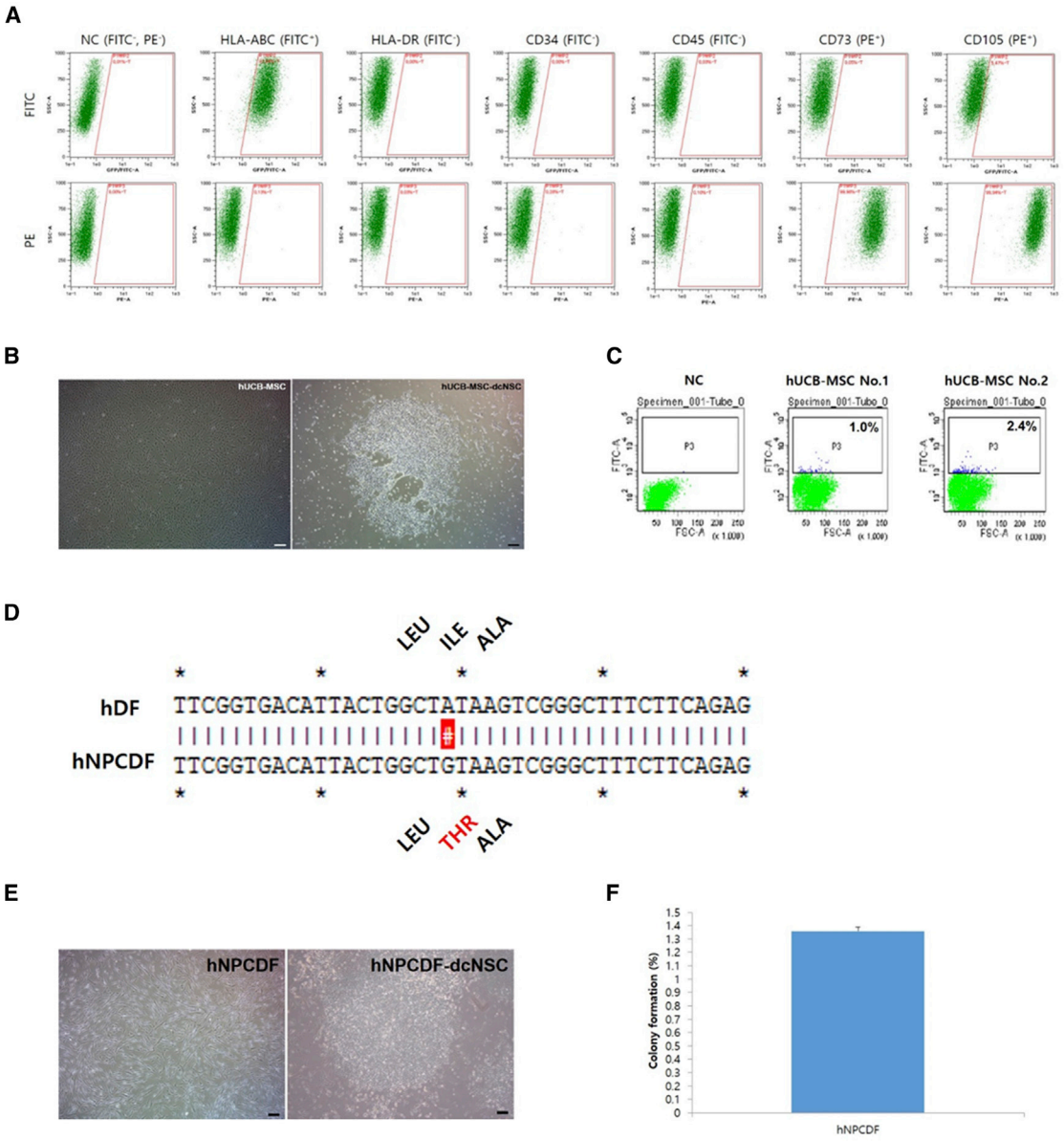

Figure 3. Generation of dcNSCs from Different Cells Using Optimized Direct Conversion Conditions

(A) Human umbilical-cord-blood-derived mesenchymal stem cells (hUCB-MSCs) that underwent direct conversion expressed a typical mesenchymal stem-cell-specific marker. (B) The fibroblastic morphology of the hUCB-MSCs changed into a dcNSC-specific phenotype following direct conversion. (C) Expression of a dcNSC-specific marker was induced with high efficiency in both hUCB-MSC batches by direct conversion. (D) Human Niemann-Pick Type C disease-derived dermal fibroblasts (hNPCDFs) that underwent direct conversion had a point mutation in their genomic DNA. (E) Fibroblastic morphology of hNPCDFs changed to dcNSC-specific morphology, following direct conversion. (F) The efficiency of direct conversion (number of colonies per initial cell number at day 14) was >1%. Scale bars, 200 μm.

proto-oncogene overexpression levels in somatic cells. The generated dcNSCs will be useful for future *in vitro* drug screening studies conducted to identify new therapeutics to treat neurological diseases. In addition, this method lowers expression levels of p53, a major reprogramming hurdle, thus allowing it to be safely used to enhance the efficiency of direct conversion into other types of target cells in the future.

MATERIALS AND METHODS

Retrovirus Production, Concentration, and Titration

For retrovirus-related experiments, our laboratory has been certified as a living modified organism research facility. The overall process of retrovirus production, concentration, and titration is illustrated in Figure 1B. To generate retroviruses, 24 μL Convoy (ACTGene, Piscataway, NJ, USA), 4 μg pMXs-hc-Myc or pMXs-hSox2, 2 μg VSV-G,

A

	Unrelated hDF		Parental hDF		hDF-dcNSC	
Sex	XX		XX		XX	
Locus	Allele 1	Allele 2	Allele 1	Allele 2	Allele 1	Allele 2
D8S1179	10	14	13	13	13	13
D21S11	31.2	32.2	28	31.2	28	31.2
D7S820	8	11	10	10	10	10
CSF1PO	11	12	11	12	11	12
D3S1358	16	16	14	16	14	16
TH01	9	9	7	7	7	7
D13S317	11	12	11	12	11	12
D16S539	9	11	12	13	12	13
D2S1338	20	23	17	21	17	21
D19S433	13	13	14	14	14	14
vWA	14	18	17	17	17	17
TPOX	11	11	8	10	8	10
D18S51	12	13	14	16	14	16
D5S818	11	13	12	13	12	13
FGA	22	23	21	26	21	26

B

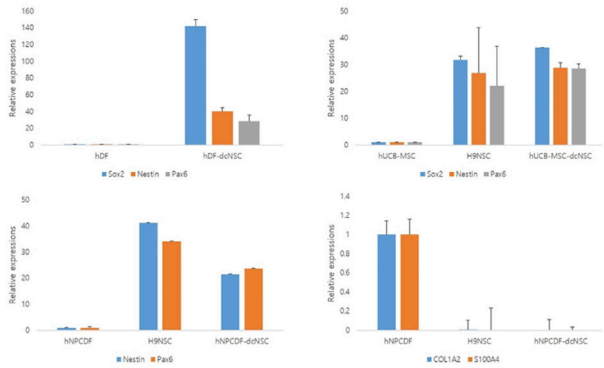

C

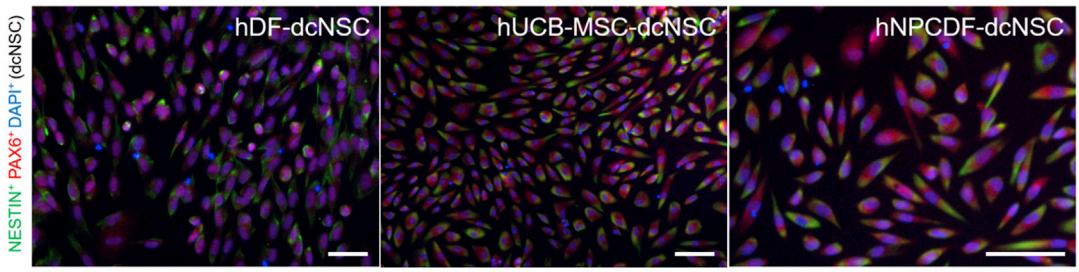

D

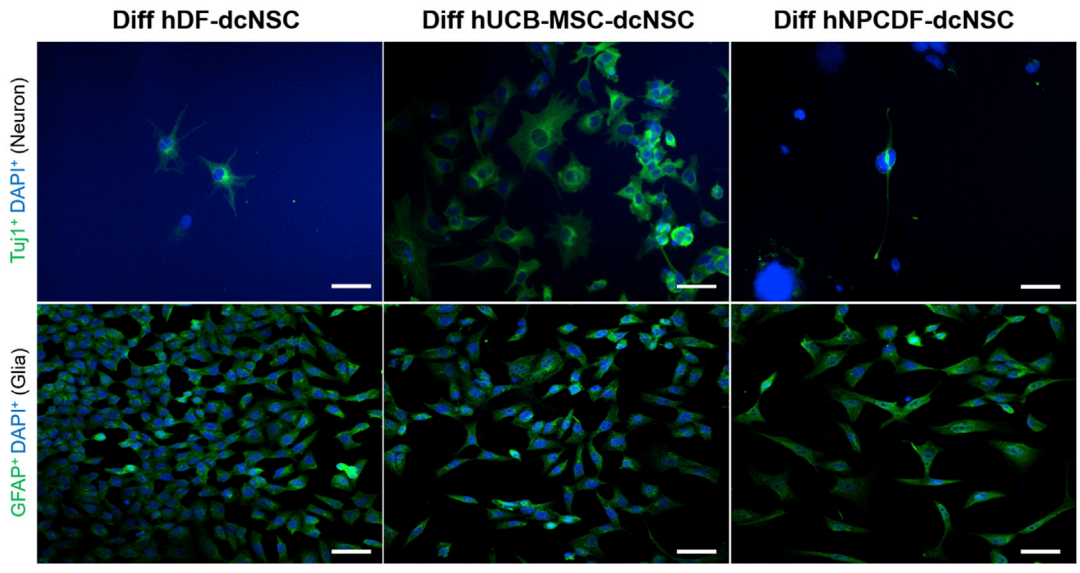

(legend on next page)

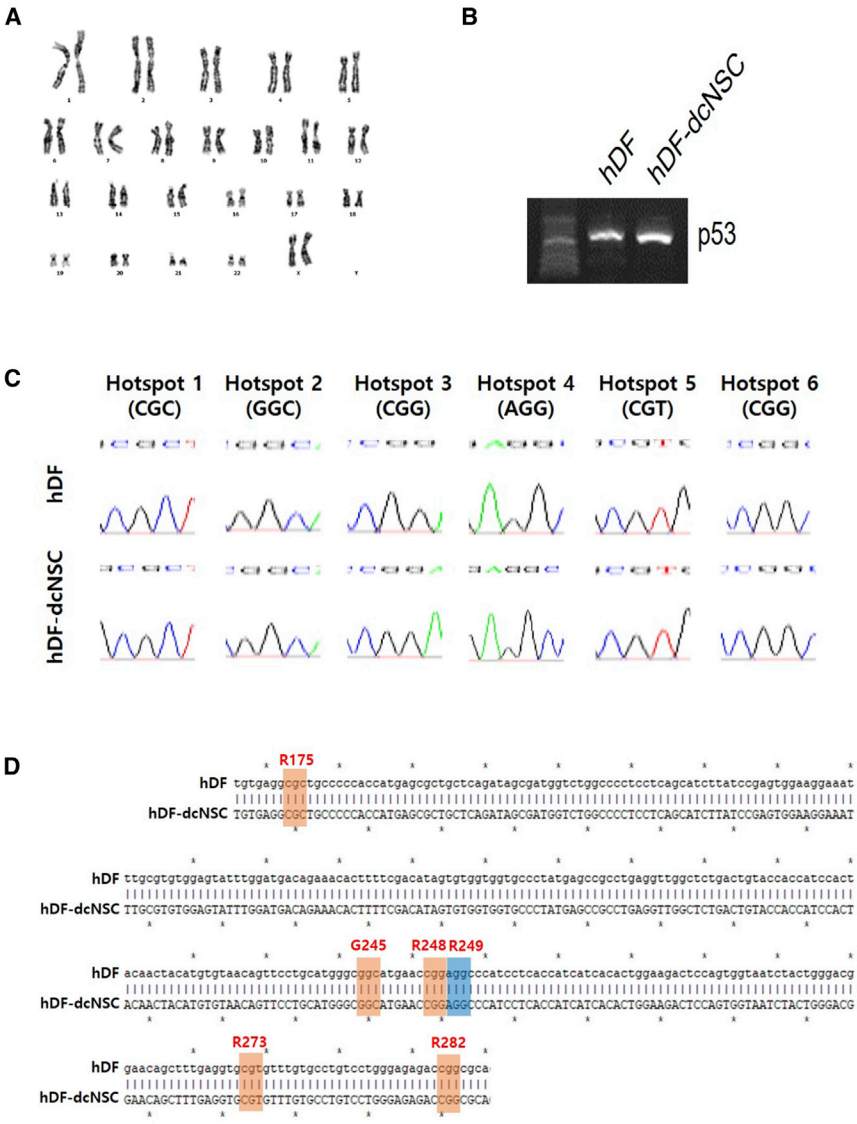

Figure 5. Characterization of *p53* Mutation Hotspot in dcNSCs

(A) The hDF-dcNSCs had a normal karyotype (46, XX) after direct conversion. (B) To identify mutations in the *p53* gene, the *p53* locus was amplified from cDNA. (C) Sequencing of the *p53* locus PCR product revealed that all 6 hotspots remained normal. (D) Sequencing of *p53* locus in multiple clones revealed that all 6 hotspots remained normal.

and 2 μg Gag-Pol were mixed and incubated at 25°C for 10 min. These mixtures were added to 2 × 10^6 293FT cells attached to a 100-mm dish and incubated overnight at 37°C in 5% CO_2. To titrate the viruses, pMXs-GFP vector was transfected in parallel under the same conditions. Virus-containing supernatants were collected at 24, 48, and 72 h post-transfection and stored at 4°C. To concentrate the viruses, virus-containing supernatants were passed through a 0.45-μm filter mixed with Retro-X concentrator (Clontech, Mountain View, CA, USA) at a 1:3 ratio of concentrator to supernatant, and incubated overnight at 4°C. After 24 h, the mixture was centrifuged at 4,000 rpm for 60 min at 4°C. The resulting supernatants were discarded, and the retrovirus-containing pellets were resuspended and dispensed in PBS (HyClone, Logan, UT, USA) and stored at −80°C until further use. To titrate the viruses, 50, 5, 0.5, and 0 μL concentrated GFP retrovirus were used to infect 5 × 10^5 293FT cells, and the proportion of GFP-positive cells was measured by flow cytometry (Miltenyi Biotec, Bergisch Gladbach, Germany) at 2 days post-infection (Figures 1C and 1D). Based on results ranging from 1% to 20%, the titers were calculated using the equation in Figure 1D.

Direct Conversion into dcNSCs

The use of human samples for cellular reprogramming was approved by the Institutional Review Board. On the day before retrovirus transduction, 1.25 × 10^4 somatic cells were plated on 24-well tissue culture plates. On the next day, MS virus was added to the cells at an MOI of 1, and spinfection was performed at 800 × *g* for 60 min at 20°C. After spinfection, the cells were incubated in DMEM/F12 (Thermo Fisher Scientific, Waltham, MA, USA) containing 20% (v/v) fetal bovine serum (Thermo Fisher Scientific) and 1× primocin (InvivoGen, San Diego, CA, USA) for 3 days. On the third day, 5 × 10^3 cells were seeded onto poly L-ornithine (Sigma, St. Louis, MO, USA)/fibronectin (Corning, Corning, NY, USA)-coated 6-well plates (Thermo Fisher Scientific). After confirming cellular attachment, the medium was replaced with dcNSC medium (StemPro NSC medium with 1× supplement, 1× primocin, 20 ng/mL basic fibroblast growth factor [bFGF], and 20 ng/mL epidermal growth factor [EGF]), which was replaced further with fresh medium once every 2 days. On days 14–21, dcNSC colonies were mechanically picked and cultured on poly L-ornithine/fibronectin-coated plates. For neurosphere cultures, the dcNSCs were

Figure 4. General Characterization of dcNSCs

(A) The hDF-dcNSCs were determined to originate from parental hDFs through fingerprinting. (B) At the mRNA level, dcNSCs generated from different sources simultaneously expressed multiple NSC-specific markers, while fibroblast markers were concurrently silenced. (C) At the protein level, dcNSCs expressed multiple NSC-specific proteins. (D) The dcNSCs generated from different sources were multipotent and could be differentiated into neurons and glia. Scale bars, 200 μm.

Table 1. Used Primers

Gene	Sequences (5′ to 3′)	Size (bp)
BAX	F-ACGAACTGGACAGTAACATGGAG	397
	R-CTTCTTCCAGATGGTGAGTGA	
COL1A2	F-ACAAGGCATTCGTGGCGATA	115
	R-ACCATGGTGACCAGCGATAC	
GAPDH	F-GTCAGTGGTGGACCTGACCT	245
	R-TGCTGTAGCCAAATTCGTTG	
GFAP	F-GCTCAATGACCGCTTTGCCAG	215
	R-CCTGTGCCAGATTGTCCCTCT	
MAP2	F-GGCAGATGAACGGAAAGATGAAGC	207
	R-GTATTTGAATAGGTGCCCTGTGACC	
NESTIN	F-GCATGTGAATGGGGGAGTGA	81
	R-TCTCCCTCAGAGACTAGCGG	
NPC1	F-ATGAGATTCCTGCCCATGTTCC	329
	R-GACACACCGAGGTTGAAGATAGTG	
OCT-4	F-GAAGGATGTGGTCCGAGTGT	183
	R-GTGAAGTGAGGGCTCCCATA	
OLIG1	F-TCCTCCACCTCCTCCACTTC	307
	R-CTATCTTGGAGAGCTTGCGGC	
p53	F-TCTGTGACTTGCACGTACTCC	586
	R-GAGAGGAGCTGGTGTTGTTGG	
PAX6	F-CAGAGAAGACAGGCCAGCAA	219
	R-TGGTTGGTAGACACTGGTGC	
REX1	F-GGCGGAAATAGAACCTGTCA	152
	R-CTTCCAGGATGGGTTGAGAA	
S100A4	F-GGGCAAAGAGGGTGACAAGT	139
	R-CCTGTTGCTGTCCAAGTTGC	
Endogeneous *SOX2*	F-GAGAGTGTTTGCAAAAGGGGG	148
	R-CGCCGCCGATGATTGTTATTA	

Note. F, forward; R, reverse.

incubated in the attached state, removed using accutase (STEMCELL Technologies, Vancouver, Canada), and subsequently resuspended in a Petri dish to allow the formation of a neurosphere (Figure 1E). The dcNSCs were slowly frozen using dcNSC medium with 5% DMSO (Sigma) and fast-thawed in a 37°C water bath (Figure 1F).

Reprogramming of iPSCs and AP Staining

Briefly, 1.25×10^4 hDF cells were plated on a 24-well tissue culture plate (Thermo Fisher Scientific) on the day before retroviral transduction. The next day, retroviral OSMK or a combination excluding one of the reprogramming factors was mixed with the cells at an MOI of 10, and spinfection was performed at 800 × *g* for 60 min at 20°C. The cells were incubated in DMEM/F12 containing 20% (v/v) fetal bovine serum and 1× primocin for 3 days and subcultured on the tissue culture plates containing STO feeder cells. From days 5–21, the medium was replaced daily with fresh iPSC medium (DMEM/F12, 20% serum replacement, 1× primocin, and 4 ng/mL bFGF). At day 21, the cells were stained with AP, and the reprogramming efficiency was calculated by counting the number of AP-positive colonies.

In Vitro Differentiation

Spontaneous differentiation of dcNSCs was induced by culturing cells in bFGF and EGF-free dcNSC medium for 3 weeks, where the medium was replaced with fresh medium every 2 to 3 days. For analysis of differentiated cells, qRT-PCR (*MAP2*, *GFAP*, and *OLIG1*) or immunofluorescence staining (TUJ1, GFAP, and OLIG2) was performed.

qRT-PCR

The primer list for qRT-PCR is presented in Table 1. The mRNA was isolated from cell pellets using a PureLink RNA Mini Kit (Thermo Fisher Scientific). cDNA was synthesized from this mRNA using the AccuPower RT Premix (Bioneer, Daejeon, South Korea). PowerUp SYBR Green Master Mix (Applied Biosystems, Foster City, CA, USA), cDNA, primer, and distilled water were combined to a final volume of 20 μL. PCR was performed using Quant Studio 3 (Applied Biosystems), and the relative fold values for each gene were calculated using the ΔΔCt method.

Immunofluorescence Staining

The cells were fixed, permeabilized, blocked, and subsequently treated overnight with either anti-NESTIN (Abcam, Cambridge, UK), anti-PAX6 (BioLegend, San Diego, CA, USA), anti-OLIG2 (Millipore, Burlington, MA, USA) or anti-TUJ1 primary antibody (Abcam), depending on the experiment, at a 1:100 dilution at 4°C. Next, the cells were washed with PBS and incubated with either Alexa 488 goat anti-mouse (Invitrogen, Waltham, MA, USA), Alexa Fluor 594 goat anti-mouse (Thermo Fisher Scientific), or Alexa Fluor 594 goat anti-rabbit (Invitrogen) secondary antibody, based on the primary antibody type, at a dilution of 1:1,000 at 25°C for 2 h. After washing the cells and removing extra secondary antibody with PBS, nuclei were stained with DAPI. Stained cells were visualized using a Nikon ECLIPSE Ti-U microscope (Nikon, Tokyo, Japan). Excitation/emission wavelengths were 358/461 nm (DAPI), 488/525 nm (Alexa 488), and 594/617 nm (Alexa Fluor 594).

Live-Cell Staining and Flow Cytometry

Live cells (10^5–10^6) were suspended in 100 μL PBS, mixed with 3 μL fluorescein isothiocyanate (FITC)-conjugated antibody, and subsequently incubated in the dark at 25°C for 30 min. The antibodies used were anti-CD133/1-VioBright/FITC (Miltenyi Biotec), anti-HLA-ABC (BD Biosciences, Franklin Lakes, NJ, USA), anti-HLA-DR (BD Biosciences), anti-CD34 (BD Biosciences), anti-CD45 (BD Biosciences), anti-CD73 (BD Biosciences), and anti-CD105 (BD Biosciences). After 30 min, the cells were washed with 3 mL PBS and analyzed using the MACSQuant VYB (Miltenyi Biotec).

Western Blot Analysis

Western blot analysis was performed as previously described by Kwon et al.[10] MS was introduced into the cells, which were sampled on day 6. Cells were treated with lysis buffer to separate the protein, and

denatured protein was obtained through boiling subsequently. Denatured proteins were separated on SDS-PAGE gels (Bio-Rad, Hercules, CA, USA), and transferred to polyvinylidene fluoride membranes (Bio-Rad). The membranes were blocked with skim milk and incubated with anti-p53 (1:1,000; Santa Cruz Biotechnology, Dallas, TX, USA) antibody at 4°C overnight. On the next day, the membranes were washed, incubated in horseradish peroxidase (HRP)-conjugated secondary antibody (1:1,000; Santa Cruz) for 1 h at 25°C, followed by another wash, and developed in enhanced chemiluminescence (ECL) solution (iNtRON Biotechnology, Gyeonggi-do, South Korea).

DNA Fingerprinting and Karyotyping

Genomic DNA of unrelated hDF, parental hDF and hDF-dcNSC was isolated using the AccuPrep Genomic DNA Extraction Kit (Bioneer). The separation method followed the manufacturer's protocol. The isolated genomic DNA was amplified using 16 human fingerprinting primer sets. The amplification was checked by electrophoresis for normality, and the fragment size was analyzed. Amplification and fragment size analysis was performed at the Korea Gene Information Center (Seoul, South Korea) (Figure 4A). Karyotyping was performed at Samkwang Medical Laboratories (Smlab; Seoul, South Korea), where 10 metaphase spreads were analyzed (Figure 5A).

Genotyping and In-Depth Genotyping

The RNA was isolated from hDFs and hDF-dcNSCs using the PureLink RNA Mini Kit (Invitrogen). The cDNA was synthesized using AccuPower RT PreMix (Bioneer). The gDNA was isolated from hNPCDFs using the AccuPrep Genomic DNA Extraction Kit (Bioneer). PCR amplification was performed in a GeneTouch Thermal Cycler (Bioer, Hangzhou, China). The resulting PCR products were separated by gel electrophoresis (Clontech) and purified using the MEGAquick-spin Plus Total Fragment DNA Purification Kit (iNtRON Biotechnology). Sequencing of purified PCR products were performed by Macrogen (Seoul, South Korea) using the primer, which was used in the original PCR. For in-depth genotyping, PCR products were cloned using the TOPcloner TA Kit (Enzynomics, Daejeon, South Korea) and transformed into chemically competent DH5α *Escherichia coli* (Enzynomics) using the heat-shock method. Transformed *E. coli* cells were spread on Luria-Bertani (LB) Agar LOP plates (Narae Biotech, Gyeonggi-do, South Korea) and incubated overnight at 37°C. On the next day, 10 colonies were inoculated into LB broth (Thermo Fisher Scientific) and incubated overnight at 37°C. Plasmids were isolated from the cultured *E. coli* using an AccuPrep Plasmid Mini Extraction Kit (Bioneer), and sequencing was performed by Macrogen.

Statistical Analysis

All data were assessed with an unpaired t test using GraphPad Prism software v4.02 (San Diego, CA, USA), where a $p < 0.01$ or $p < 0.05$ was considered significant.

SUPPLEMENTAL INFORMATION

Supplemental Information includes two figures and can be found with this article online at https://doi.org/10.1016/j.omtn.2018.12.009.

AUTHOR CONTRIBUTIONS

K.D., S.K.-W., and K.K.-S., designed the experiments, analyzed the data, and wrote the manuscript. K.D., H.M.-J., J.M., and A.H.-J. conducted the experiments. All authors read and approved the final version of the manuscript.

CONFLICTS OF INTEREST

The authors declare no potential conflicts of interest.

ACKNOWLEDGMENTS

This work was supported by National Research Foundation of Korea (NRF) grants funded by the Korean government (MSIT) (2016K1A3A1A61006001 and 2016R1C1B1010742).

REFERENCES

1. Nussbaum, R.L., and Ellis, C.E. (2003). Alzheimer's disease and Parkinson's disease. N. Engl. J. Med. *348*, 1356–1364.
2. Katara, P. (2014). Single nucleotide polymorphism and its dynamics for pharmacogenomics. Interdiscip. Sci. *6*, 85–92.
3. Avior, Y., Sagi, I., and Benvenisty, N. (2016). Pluripotent stem cells in disease modelling and drug discovery. Nat. Rev. Mol. Cell Biol. *17*, 170–182.
4. Kwon, D., Ji, M., Lee, S., Seo, K.W., and Kang, K.S. (2017). Reprogramming enhancers in somatic cell nuclear transfer, iPSC technology, and direct conversion. Stem Cell Rev. *13*, 24–34.
5. Vierbuchen, T., Ostermeier, A., Pang, Z.P., Kokubu, Y., Südhof, T.C., and Wernig, M. (2010). Direct conversion of fibroblasts to functional neurons by defined factors. Nature *463*, 1035–1041.
6. Yu, K.R., Shin, J.H., Kim, J.J., Koog, M.G., Lee, J.Y., Choi, S.W., Kim, H.S., Seo, Y., Lee, S., Shin, T.H., et al. (2015). Rapid and efficient direct conversion of human adult somatic cells into neural stem cells by HMGA2/let-7b. Cell Rep. *10*, 441–452.
7. Takahashi, K., and Yamanaka, S. (2006). Induction of pluripotent stem cells from mouse embryonic and adult fibroblast cultures by defined factors. Cell *126*, 663–676.
8. Takahashi, K., Tanabe, K., Ohnuki, M., Narita, M., Ichisaka, T., Tomoda, K., and Yamanaka, S. (2007). Induction of pluripotent stem cells from adult human fibroblasts by defined factors. Cell *131*, 861–872.
9. Araki, R., Hoki, Y., Uda, M., Nakamura, M., Jincho, Y., Tamura, C., Sunayama, M., Ando, S., Sugiura, M., Yoshida, M.A., et al. (2011). Crucial role of c-Myc in the generation of induced pluripotent stem cells. Stem Cells *29*, 1362–1370.
10. Kwon, D., Kim, J.S., Cha, B.H., Park, K.S., Han, I., Park, K.S., Bae, H., Han, M.K., Kim, K.S., and Lee, S.H. (2016). The effect of fetal bovine serum (FBS) on efficacy of cellular reprogramming for induced pluripotent stem cell (iPSC) generation. Cell Transplant. *25*, 1025–1042.
11. Giorgetti, A., Marchetto, M.C., Li, M., Yu, D., Fazzina, R., Mu, Y., Adamo, A., Paramonov, I., Cardoso, J.C., Monasterio, M.B., et al. (2012). Cord blood-derived neuronal cells by ectopic expression of Sox2 and c-Myc. Proc. Natl. Acad. Sci. USA *109*, 12556–12561.
12. Zou, Q., Yan, Q., Zhong, J., Wang, K., Sun, H., Yi, X., and Lai, L. (2014). Direct conversion of human fibroblasts into neuronal restricted progenitors. J. Biol. Chem. *289*, 5250–5260.
13. Winiecka-Klimek, M., Smolarz, M., Walczak, M.P., Zieba, J., Hulas-Bigoszewska, K., Kmieciak, B., Piaskowski, S., Rieske, P., Grzela, D.P., and Stoczynska-Fidelus, E. (2015). SOX2 and SOX2-MYC reprogramming process of fibroblasts to the neural stem cells compromised by senescence. PLoS ONE *10*, e0141688.
14. Peh, G.S., Lang, R.J., Pera, M.F., and Hawes, S.M. (2009). CD133 expression by neural progenitors derived from human embryonic stem cells and its use for their prospective isolation. Stem Cells Dev. *18*, 269–282.
15. Coskun, V., Wu, H., Blanchi, B., Tsao, S., Kim, K., Zhao, J., Biancotti, J.C., Hutnick, L., Krueger, R.C., Jr., Fan, G., et al. (2008). CD133+ neural stem cells in the ependyma of mammalian postnatal forebrain. Proc. Natl. Acad. Sci. USA *105*, 1026–1031.

16. Haus, D.L., Nguyen, H.X., Gold, E.M., Kamei, N., Perez, H., Moore, H.D., Anderson, A.J., and Cummings, B.J. (2014). CD133-enriched Xeno-Free human embryonic-derived neural stem cells expand rapidly in culture and do not form teratomas in immunodeficient mice. Stem Cell Res. (Amst.) *13*, 214–226.

17. Kerosuo, L., Piltti, K., Fox, H., Angers-Loustau, A., Häyry, V., Eilers, M., Sariola, H., and Wartiovaara, K. (2008). Myc increases self-renewal in neural progenitor cells through Miz-1. J. Cell Sci. *121*, 3941–3950.

18. Albrechtsen, N., Dornreiter, I., Grosse, F., Kim, E., Wiesmüller, L., and Deppert, W. (1999). Maintenance of genomic integrity by p53: complementary roles for activated and non-activated p53. Oncogene *18*, 7706–7717.

19. Lane, D.P. (1992). Cancer. p53, guardian of the genome. Nature *358*, 15–16.

20. Kim, K.Y., Hysolli, E., and Park, I.H. (2012). Reprogramming human somatic cells into induced pluripotent stem cells (iPSCs) using retroviral vector with GFP. J. Vis. Exp. *62*, e3804.

21. Kim, J.B., Zaehres, H., Araúzo-Bravo, M.J., and Schöler, H.R. (2009). Generation of induced pluripotent stem cells from neural stem cells. Nat. Protoc. *4*, 1464–1470.

22. Huangfu, D., Osafune, K., Maehr, R., Guo, W., Eijkelenboom, A., Chen, S., Muhlestein, W., and Melton, D.A. (2008). Induction of pluripotent stem cells from primary human fibroblasts with only Oct4 and Sox2. Nat. Biotechnol. *26*, 1269–1275.

23. Kidder, B.L. (2014). Generation of induced pluripotent stem cells using chemical inhibition and three transcription factors. Methods Mol. Biol. *1150*, 227–236.

24. Hong, H., Takahashi, K., Ichisaka, T., Aoi, T., Kanagawa, O., Nakagawa, M., Okita, K., and Yamanaka, S. (2009). Suppression of induced pluripotent stem cell generation by the p53-p21 pathway. Nature *460*, 1132–1135.

25. Jiang, H., Xu, Z., Zhong, P., Ren, Y., Liang, G., Schilling, H.A., Hu, Z., Zhang, Y., Wang, X., Chen, S., et al. (2015). Cell cycle and p53 gate the direct conversion of human fibroblasts to dopaminergic neurons. Nat. Commun. *6*, 10100.

26. Zhou, D., Zhang, Z., He, L.M., Du, J., Zhang, F., Sun, C.K., Zhou, Y., Wang, X.W., Lin, G., Song, K.M., et al. (2014). Conversion of fibroblasts to neural cells by p53 depletion. Cell Rep. *9*, 2034–2042.

27. Bullock, A.N., Henckel, J., DeDecker, B.S., Johnson, C.M., Nikolova, P.V., Proctor, M.R., Lane, D.P., and Fersht, A.R. (1997). Thermodynamic stability of wild-type and mutant p53 core domain. Proc. Natl. Acad. Sci. USA *94*, 14338–14342.

28. Mello, S.S., and Attardi, L.D. (2013). Not all p53 gain-of-function mutants are created equal. Cell Death Differ. *20*, 855–857.

29. Muller, P.A., and Vousden, K.H. (2013). p53 mutations in cancer. Nat. Cell Biol. *15*, 2–8.